CHAPTER 4

INVERSE MODELING AND ANALYSIS OF SOFC–GT–ST CYCLE

4.1 Introduction

The thermodynamic model of the SOFC–GT–ST cycle described in the previous chapter can be referred to as the forward model. The component wise modeling of the topping SOFC–GT and bottoming ST cycle was described in detail in chapter 3. As such, the forward/direct model described in chapter 3 is concerned with the determination of SOFC voltage, current, power, GT power, ST power, energy and exergy efficiencies, component and total system irreversibility under steady state operation for a known set of input parameters. These input operating parameters in case of the SOFC–GT–ST plant were the FFR, fuel and air properties, AFR, SOFC operating pressure, current density, geometric features and properties of the SOFC component materials, HRSG pressure/boiler pressure (BP), ST inlet superheated steam temperature (STIT) etc. However, during plant operation, sometimes, it may so happen that the performance parameters such as net power and efficiency are available, but some operating parameters are not known. The correct prediction of the unknown operating parameters requires the solution of a problem which is usually referred to as the inverse problem. But otherwise also, the inverse method is useful in finding operating parameters against some set objectives of designed performance criteria.

In recent years, inverse techniques are successfully applied in a wide range of engineering problems [1, 2, 3-8] for estimating system parameters. For example in heat transfer problems, temperature measurements with thermocouple are possible however the boundary temperature or the boundary heat flux may not be known. Prediction of unknown boundary temperature or the boundary heat flux constitutes a classical inverse heat transfer problem [9]. Inverse analysis can also be used for the characterization of the unknown material properties. Unfortunately, it has not been applied to predict or estimate parameters of SOFC integrated power systems including that of SOFC–GT–ST system.

In chapter 1, a brief introduction about the definition of inverse problem and its importance was provided. Usually solution of an inverse problem requires the use of an

optimization technique but it is not similar to a normal optimization study. In regular single/multiple objective optimization problems, the objective functions are either maximized or minimized simultaneously and accordingly the decision variables are selected for its optimum solution. Whereas, in an inverse analysis, the parameters are estimated against known values of the system performance parameters (objective functions). Therefore, the inverse method although it uses an optimization technique but it's purpose is totally different from that of a normal optimization problem.

A differential evolution (DE) based search algorithm is used in this study to estimate six unknown operating parameters viz. the FFR, additional FFR, AFR, current density, HRSG pressure/BP and the STIT of the SOFC integrated combined cycle (CC) power plant. Evolutionary based search techniques are usually suitable for nonlinear/discontinuous objective functions and hence, they are preferred over the conventional deterministic methods [10]. The plant's net power, efficiencies (energy and exergy) and total system irreversibility are the objective functions in the present inverse problem; initially a single objective function is considered at a time for estimation of the operating parameters. In another attempt, the values of the all the four objective functions are considered known and the unknown operating parameters are estimated simultaneously.

4.2 Differential evolution (DE) based inverse method

In the inverse problem, as stated above, the plant's operating parameters such as FFR, additional FFR, AFR, SOFC current density, HRSG pressure, STIT are assumed to be unknowns and it is attempted to estimate these parameters simultaneously corresponding to the net power ($\dot{W}_{net,CC}$),energy efficiency (η_I), exergy efficiency (η_{II}) and the total system irreversibility ($\dot{I}$) values obtained from the plant simulation of the SOFC–GT–ST system (forward problem). Initially, it starts with some random arbitrary values of the unknowns. Power, efficiencies and total system irreversibility corresponding to the arbitrary values of the unknowns is determined. Then the square of the error between the exact value and the new value evaluated based on arbitrary values of the unknowns is minimized and updated in an iterative manner until the convergence criteria is fulfilled. This is mathematically represented in the following manner:

$$f_1 = \sqrt{\left(\dot{W}_{net,CC} - \tilde{\dot{W}}_{net,CC}\right)^2} \tag{4.1}$$

$$f_2 = \sqrt{\left(\eta_I - \tilde{\eta}_I\right)^2} \tag{4.2}$$

$$f_3 = \sqrt{\left(\eta_{II} - \tilde{\eta}_{II}\right)^2} \tag{4.3}$$

$$f_4 = \sqrt{\left(\dot{I} - \tilde{\dot{I}}\right)^2} \tag{4.4}$$

In case of parameter estimation corresponding to the four known objective function parameter values, the following fitness function is used to estimate the six unknown operating parameters.

$$f_5 = \sqrt{\left[\left(\frac{\dot{W}_{net,CC} - \tilde{\dot{W}}_{net,CC}}{\tilde{\dot{W}}_{net,CC}}\right)^2 + \left(\frac{\eta_I - \tilde{\eta}_I}{\tilde{\eta}_I}\right)^2 + \left(\frac{\eta_{II} - \tilde{\eta}_{II}}{\tilde{\eta}_{II}}\right)^2 + \left(\frac{\dot{I} - \tilde{\dot{I}}}{\dot{I}}\right)^2\right]} \tag{4.5}$$

In the above equations, $\tilde{\dot{W}}_{net,CC}$, $\tilde{\eta}_I$, $\tilde{\eta}_{II}$ and $\tilde{\dot{I}}$ are the net power, energy efficiency, exergy efficiency and total system irreversibility corresponding to the arbitrary values of the unknowns. For minimizing the fitness functions (f_1, f_2, f_3, f_4, f_5), a DE based optimization algorithm is used in the present work. In the DE based search method, the searching range of parameters is specified and some arbitrary values of the unknown operating parameters are randomly chosen from the range of specified parameter values. The optimization process is terminated when the fitness function (f) attains a minimum prescribed value during the course of multiple iterations/generations. The termination condition in the present analysis is however the number of iterations/generations which is specified in the program.

DE algorithm is considered as one of the most powerful evolutionary algorithms for real valued function optimization. Storn and Price [11] first proposed DE as one of the evolutionary optimization algorithms. It belongs to the class of genetic algorithms (GAs) which use biology−inspired operations of mutation, crossover and selection on a population in order to minimize the fitness function over the course of successive generations [12]. Many engineering problems contain objective functions that are highly

non-linear, non-differentiable, non-continuous and multidimensional having many local minima, constraints or stochasticity. Such problems which are otherwise difficult to optimize/solve can be optimized/solved using evolutionary algorithms such as DE [3]. Initialization, mutation, recombination (crossover) and selection are the four basic operations associated with DE algorithm. During initialization, the population size and lower and upper bounds of the parameters to be estimated are specified. Next, the parameter vector is generated randomly and uniformly within the search space from the defined lower and upper bounds of the parameters. After this, the mutation, crossover, and the selection operations are performed which are repeated generation after generation until the specified number of generations is completed. Over the course of successive generations, the fitness function shown in equations (4.1) to (4.5) is minimized and this completes the estimation of the unknown parameters. For the details on DE algorithm, one can refer to the articles mentioned in references. [13, 14]. Fig. 4.1 shows a typical evolutionary scheme. Initialization, mutation, recombination (crossover) and selection are the four basic operations associated with such algorithm.

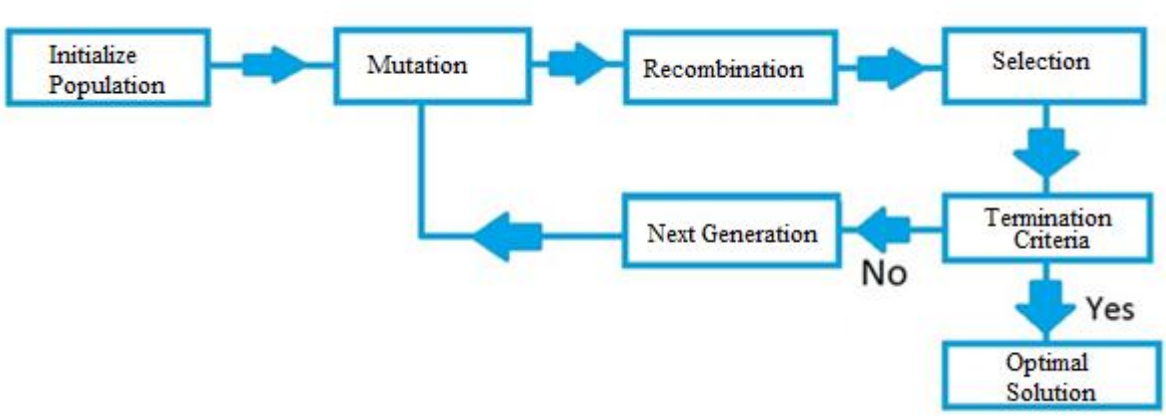

Fig. 4.1: General Evolutionary Algorithm Procedure

4.2.1 Initialization [14]

During initialization, the population size is selected depending on the mutation strategy used and nature of the objective function. The parameter vectors can be expressed in the form:

$$X_{i,G} = \left[X^{1}_{i,G}; X^{2}_{i,G}; \ldots\ldots; X^{D}_{i,G}\right];\ i = 1,2,\ldots\ldots, NP \qquad (4.6)$$

The parameter vector is also called the target vector. In Eq. (13), *D* is the number of parameters, *NP* is the population size and *G* is the generation number. Next, the lower and upper bounds for each parameter are defined as follows:

$$X^{j}_{\min} \le X^{j}_{i,0} \le X^{j}_{\max};\ j = 1,2,.....,D \tag{4.7}$$

The initial population should cover the entire search space as much as possible. This is done through random selection of initial parameter values uniformly within the search space from the defined lower and upper bounds of the parameters. For example, the initial value of the j^{th} parameter of the i^{th} individual at generation G=0 is generated as follows [12]:

$$X^{j}_{i,0} = X^{j}_{\min} + rand \in (0,1)\left(X^{j}_{\max} - X^{j}_{\min}\right) j = 1, 2, \ldots, \mathrm{D} \tag{4.8}$$

where $rand \in (0,1)$ represents a uniformly distributed random variable within the range [0, 1]. Various ranges of *NP* values such as 5D to 10D, 3D to 8D and 2D to 40D are suggested for different optimization problems to adjust the convergence speed and reliability of DE [15]. The reasonable choice for *NP* is between 5D and 10D but NP must be at least 4 in DE/rand/1/bin (the basic mutation strategy proposed by Storn and Price [11]) to ensure that DE has enough mutually different vectors. The larger the population size, the higher the probability of finding a global optimum for multi-modal problems. But, a larger population also slows down the convergence demanding a large number of function evaluations. Therefore, smaller population size is recommended for separable and uni-modal functions to speed up the convergence, while larger populations (10D or higher) for parameter-linked multi-modal functions to avoid premature convergence.

4.2.2 Mutation [14]

After initialization, DE employs the mutation operation to produce a mutant vector $V_{i,G}$ with respect to each parameter $X_{i,G}$. Through the mutation operation, the search space is expanded. A number of mutation strategies are proposed e.g. DE/rand/1/bin, DE/rand/2/bin, DE/best/1/bin, DE/best/2/bin, DE/rand-to-best/1/bin, DE/rand-to-best/2/bin, DE/target-to-best/1/bin, DE/target-to-best/2/bin, DE/current-to-rand/1/bin. Relative merits and demerits of all these mutation strategies are discussed along with their mathematical representation in the reference [15]. For more details about

these mutation strategies one can refer to the reference [15] and the other source articles which are also referred in [15]. However, the classical DE proposed by Price and Storn [11] uses DE/rand/1/bin which is most widely used [15]. This mutation strategy is used in the present study. In DE/rand/1/bin, the mutant vector $V_{i,G} = \{V_{i,G}^1, V_{i,G}^2, V_{i,G}^3, ...V_{i,G}^D\}$ corresponding to each target vector $X_{i,G}$ is generated using the following equation [3, 4, 11, 15].

$$V_{i,G} = X_{r1,G} + F(X_{r2,G} - X_{r3,G}) \tag{4.9}$$

$V_{i,G}$ is also called the donor vector. The above equation used in the mutation operation generates new parameter vectors by adding the weighted difference of two population vectors $(X_{r2,G}, X_{r3,G})$ with a third vector $X_{r1,G}$. In this equation, r_1, r_2 and r_3 are three mutually different integer vectors randomly selected within the range [1, *NP*] for each mutant vector. The integers r_1, r_2 and r_3 are also chosen to be different from the running index i. Therefore it requires that the population size NP must be greater or equal to 4 to allow for this condition. F is called the scale factor (also known as mutation factor), a positive control parameter which controls the amplification of the difference vector $(X_{r2,G} - X_{r3,G})$. The most common value of F is usually chosen in the range [0.4, 1], F smaller than 0.4 and greater than 1.0 are only occasionally effective; however effective values are typically less than one [11,15,16]. F=1.0 is not recommended since it reduces the number of potential trial solutions and may lead to stagnation [15]. Various researchers have proposed different values for F. A larger F (but less than 1) is usually faster, reliable and it also increases the probability of escaping from a local optimum. F must be higher to avoid premature convergence and sub-optimal solution, but at the same if it becomes too large, the number of function evaluations required to find the optimum parameters also grows very quickly [15].

4.2.3 Recombination [14]

After the mutation phase, recombination is performed to develop a trial vector, $U_{i,G} = \{U_{i,G}^1, U_{i,G}^2, U_{i,G}^3, ...U_{i,G}^D\}$ by mixing the elements of the target vector $X_{i,G}$ and the donor vector $V_{i,G}$. This is referred to as "crossover" in evolutionary algorithm where

successful solutions from the previous generation are mixed with the current donors. Crossover is a uniform binomial operation as defined below [11, 15, 17]:

$$U_{i,G}^{j} = \begin{Bmatrix} V_{i,G}^{j} & \text{if } (\text{rand}_{\text{j}}^{\text{i}} \in [0,1] \le \text{CR}) \text{ or } (\text{j} = \text{I}_{\text{rand}}) \\ X_{i,G}^{j} & \text{if } (\text{rand}_{\text{j}}^{\text{i}} \in [0,1] > \text{CR}) \text{ and } (\text{j} \ne \text{I}_{\text{rand}}) \end{Bmatrix} \text{j} = 1, 2, \ldots, \text{D}; \text{i} = 1, 2, \ldots..\text{NP} \qquad (4.10)$$

In Eq. (4.10), CR is the crossover rate which is a user-defined constant in the range [0, 1]. It controls the fraction of parameter values in the trial vector to be copied from the mutant vector. No crossover (CR = 0) means whole new generation (offspring) is made from exact copies of chromosomes of the old population (parents); however, it does not mean that the new generation is the same as that of the old population. Crossover is made in the hope that new chromosomes will have good parts of old chromosomes and better than the old chromosomes. Crossover with CR = 1.0 implies all offspring are made by crossover from parts of parents' chromosome. However, a general practice is to allow some part of population survive to next generation because when CR = 1.0 is chosen, the number of trial solutions may sometime reduce dramatically leading to stagnation [15]**.** A good choice for CR is between 0.3 and 0.9, however for parameter dependent problems, CR in the range (0.9, 1.0) is the best [15, 17]. A large CR usually speeds up the convergence. I_{rand} in Eq. (17) is a randomly chosen integer in the range [1, D]. The binomial crossover operator copies the j^{th} parameter of the mutant vector $V_{i,G}^{j}$ to the corresponding element in the trial vector $U_{i,G}^{j}$ if $\text{rand}_{\text{j}}^{\text{i}} \in [0,1] \le \text{CR}$ or $\text{j} = \text{I}_{\text{rand}}$. Otherwise, it is copied from the corresponding target vector $X_{i,G}$ [17]. The condition $\text{j} = \text{I}_{\text{rand}}$ is implemented to ensure that the trial vector $U_{i,G}^{j}$ is different from its corresponding target vector $X_{i,G}$ by at least one parameter.

4.2.4 Selection [14]

Next the objective function values of all trial vectors are evaluated and compared with that of the corresponding target vector $X_{i,G}$ in the current population. If the trial vector yields a lower or equal objective function value than the corresponding target vector, the trial vector will replace the target vector and enter the population of the next

generation. Otherwise, the target vector will remain in the population for the next generation. This operation is called selection as expressed as follows [18]:

$$X_{i,G+1} = \begin{Bmatrix} U_{i,G} & \text{if } f(U_{i,G}) \leq f(X_{i,G}) \\ X_{i,G} & \text{Otherwise} \end{Bmatrix} \tag{4.11}$$

The above three operations of mutation, crossover and selection are repeated generation after generation until the termination condition is satisfied. The termination condition in the present case is the number of generation. The number of generation is specified in the coupled forward model−DE based inverse program and parameters are estimated from the inverse analysis. The flow chart of DE algorithm is presented in Fig. 4.2.

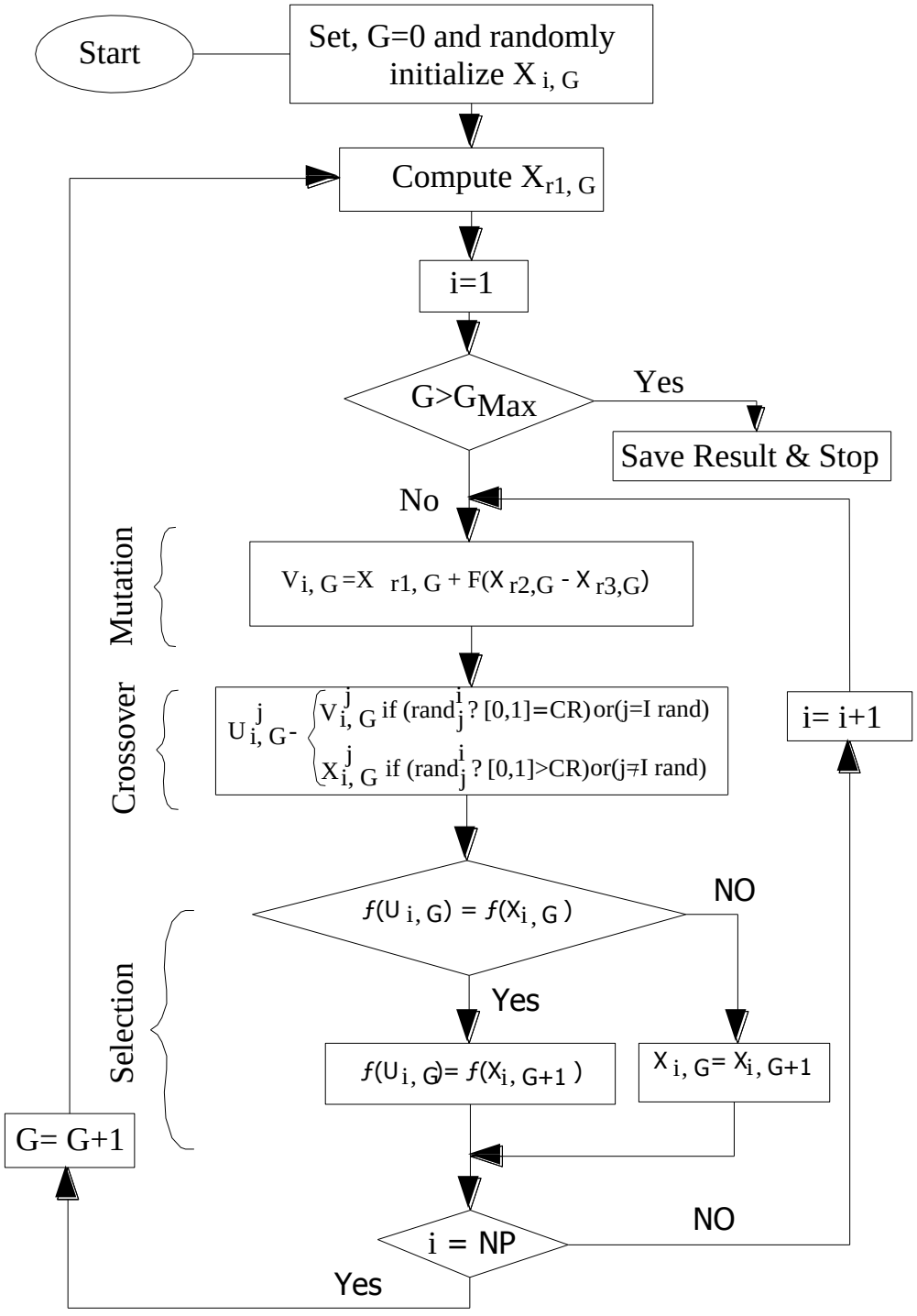

Fig. 4.2: Flow chart of the DE Algorithm

4.3 Estimation of operating parameters of SOFC integrated combined cycle plant

The simulated performance of the proposed SOFC–GT–ST plant (Fig. 3.1 Chapter 3) under various operating conditions was discussed in chapter 3. A detailed parametric analysis based on variation of CPR, FFR, additional FFR, AFR, SOFC current density, HRSG/boiler pressure (BP) and STIT was also provided in the previous chapter. From the parametric analysis, it was found that the total power and efficiencies (energy and exergy) of the SOFC–GT–ST system increases with CPR and the system performs efficiently at higher CPR producing less total irreversible losses. Similar CPR based performance variation of SOFC–GT systems is available in articles [19,20]. It was also found that the majority of the total power is produced by the SOFC; the GT and the ST in an average, share only 25.8% and 7.5% of the total power respectively. This is a usual phenomenon with hybrid SOFC–GT–ST system as reported in previous studies [21, 22]. Performance variation with FFR showed positive impact of FFR on net power and efficiency, however with simultaneous increase in exergy destruction in the system components; a variation that is similar to the one reported in reference [20]. Increased AFR and current density has negative impact on SOFC–GT system performance which was also observed in our previous analysis presented in chapter 3. Similarly, when the STIT was increased, it was found that the SOFC and the ST plant produces more power and less total irreversibility, hence the plant's overall efficiency was more at higher STIT. This is obvious and a known trend in a ST based power plant [23], but higher STIT also caused an increase in the SOFC power. These results of net power, total system irreversibility, energy and exergy efficiency obtained from the plant simulation at CPR 6 and 14 are shown in Table 4.1 and these were obtained with or system input parameters shown in Table 4.2. The results concerning estimation of unknown parameters using the DE based inverse method are discussed in the following paragraphs.

For the DE search algorithm, a population size of 60, crossover probability of 0.7, scaling factor of 0.8 and 100 generations are considered for estimation of the six unknown parameters (FFR, additional FFR, AFR, SOFC current density, BP and STIT). The estimations are done against each pair of total powers (48.85 MW and 54.30 MW), energy efficiencies (53.607% and 59.522%), exergy efficiencies (52.120% and 57.771%)

and total system irreversibility(41.609 MW and 36.384 MW) which correspond to forward plant simulation results at CPR of 6 and 14 respectively (Table 4.1).

Table 4.1: Power, efficiency and component irreversibility of the SOFC–CC system at CPR 6 and 14

CPR	6	14
SOFC power (MW)	27.246	29.107
Net GT power (MW)	15.473	20.230
Net ST power (MW)	6.131	4.964
Total net power (MW)	48.850	54.300
Energy efficiency (%)	53.607	59.522
Exergy efficiency (%)	52.120	57.771
Irreversibility (MW)		
HRSG	3.828	3.561
ST	0.846	0.869
COND	0.199	0.191
BFP	0.457	0.431
PR	4.133	4.001
SOFC	20.644	15.806
CC	8.399	8.319
GT	0.622	0.956
FR	0.490	0.483
AR	0.629	0.087
FC	0.055	0.081
AC	0.621	0.914
Exhaust	0.684	0.685
Total irreversibility	41.609	36.384

Table 4.2: Assumed values of parameters

Parameter	Value
Fuel flow rate	300 kmol/h
Additional fuel flow rate	100 kmol/h
Fuel heating value	802000 kJ/kmol
Fuel chemical exergy	830174.37 kJ/kmol
Air flow rate	4500 kmol/h
Compressor pressure ratio	6 and 14
Fuel utilization factor	0.85
Oxygen utilization factor	0.25
Steam to carbon ratio	2.5
SOFC current density	0.3 A/cm^2
Compressor isentropic efficiency	85%
GT isentropic efficiency	85%
Combustion efficiency	95%
Generator efficiency	90%
Recuperator (AR and FR) effectiveness	75%
Recuperator pressure drop (AR and FR)	4%
SOFC pressure drop	4%
Combustor pressure drop	5%
HRSG pressure/Boiler pressure (BP)	40 bar
Steam turbine inlet temperature (STIT)	600°C
Condenser pressure	0.05 bar

Source: Ref. [24] for pressure drop values

4.3.1 Parameter estimation against a single objective function (Net power output)

Table 4.3 shows various combinations of unknown parameters estimated during five various test runs corresponding to the total power output of 48.85 MW and 54.30 MW at CPR 6 and 14 respectively. The searching ranges of different unknowns are indicated in Table 4.3.

Table 4.3: The values of estimated operating parameters (HRSG pressure, FFR, addl. FFR, AFR, STIT and current density) during five various test runs corresponding to the net power output of 48.85 MW and 54.30MW at CPR 6 and 14 respectively.

Searching Range: [35–60; 275–325; 50–100; 4500–5500; 425–625; 0.1–0.5]

CPR	Runs	BP (bar)	FFR (kmol/h)	Addl. FFR (kmol/h)	AFR (kmol/h)	STIT (°C)	Current density (A/cm^2)	New energy efficiency (%)	New exergy efficiency (%)	New irreversibility (MW)
6	Run1	58.88	286.730	141.070	5493.30	566.42	0.179	50.057	48.678	48.029
	Run2	50.74	306.856	115.878	4747.77	519.08	0.351	50.663	49.257	47.059
	Run3	53.50	315.296	120.738	4880.53	527.16	0.447	49.065	47.717	50.159
	Run4	35.89	306.630	148.565	4968.14	447.59	0.438	46.924	45.652	53.881
	Run5	50.33	306.119	95.262	5035.84	572.10	0.235	53.547	52.046	42.008
14	Run1	45.06	298.05	136.51	5332.57	497.59	0.278	54.663	53.078	44.012
	Run2	45.05	310.771	88.183	4864.13	570.36	0.232	59.754	57.986	36.170
	Run3	51.48	324.894	107.434	5298.26	504.16	0.418	54.988	53.378	43.884
	Run4	53.55	311.884	98.139	5188.19	444.93	0.163	58.151	56.405	38.827
	Run5	53.07	301.676	108.795	4823.10	532.60	0.259	57.993	56.283	39.020

As can be seen from Table 4.3, the estimated parameters are within the investigated range and different combinations of parameters are obtained that satisfy the objective function values of 48.85 MW at CPR 6 and 54.30 MW at CPR 14 separately. New efficiency (energy and exergy) and total system irreversibility values obtained from the original MATLAB code using the estimated parameters change due to estimated parameters being different from their exact values. In case of parameter estimation corresponding to net power output of 48.85 MW at CPR 6, all combinations of estimated parameters obtained during Run1 to Run5 give lower efficiencies than exact energy and exergy efficiency values of 53.607% and 52.120% at CPR 6 (see Table 4.1). The new total system irreversibility reproduced with different combinations of parameters have also higher values than the exact total irreversibility value of 41.609 MW. Amongst the five different combinations of parameters corresponding to total power (48.85 MW) at CPR 6, the parameters obtained during Run5 is comparatively better than the others. The new energy and exergy efficiencies obtained with estimated parameters during Run5 are more while total system irreversibility is less compared to the others. As an example, the iterative variation of the objective function and the operating parameters estimated during Run5 is shown in Figs. 4.3 (a-g).

Similarly in estimations corresponding to net power 54.30 MW at CPR 14, the estimated combinations of parameters during Run1, Run3, Run4 and Run5 are such that they reproduce lower energy and exergy efficiencies than their exact values. The new total system irreversibility values with respect to these estimated parameters during Run1, Run3, Run4 and Run5 are also higher than the exact value of 36.384 MW. The new total system irreversibility with estimated parameters corresponding to Run2 is however less than the exact total system irreversibility. New energy and exergy efficiency values reproduced with these parameters are also slightly higher than their exact values (59.522% and 57.771%). More interestingly, the net power of 54.30 MW is attained with these estimated parameters not only with slightly higher energy and exergy efficiencies but also with lower total system irreversibility (36.170 MW). Figs. 4.4 (a-g) present the iterative variation of the objective function and the operating parameters estimated during Run2.

4.3.2 Parameter estimation against a single objective function (Energy efficiency)

Parameters estimated during various test runs corresponding to energy efficiencies at CPR 6 (53.607%) and 14 (59.522%) are shown in Table 4.4. It was observed that in both the estimations, the energy efficiency values are exactly satisfied within 100 generations, however the new net power values reproduced from parameters estimated during Run2, Run3 and Run4 corresponding to 53.607%at CPR 6 reduce from the exact net power value (48.5 MW). The estimated parameters during Run1 and Run5 however, reproduce total power of 52.796 MW and 51.269 MW respectively and these are 8.86% and 5.71% more than its exact value. New exergy efficiencies reproduced from these estimations are however marginally less compared to its exact value (52.12%) corresponding to CPR 6. This has happened basically due to the combination of the parameters. As it was seen that the total FFRs (sum of FFR and additional FFR) estimated during Run1 and Run5 are comparatively more compared to those of Run2, Run3 and Run4. Moreover estimated AFRs during Run1 and Run5 are also relatively less. It was mentioned in Chapter 3 that increase in FFR without a proportionate increase in AFR causes an increase in SOFC stack temperature and SOFC power output. The net GT power also increases with FFR due to increase in GT inlet temperature caused by increase in SOFC stack temperature.

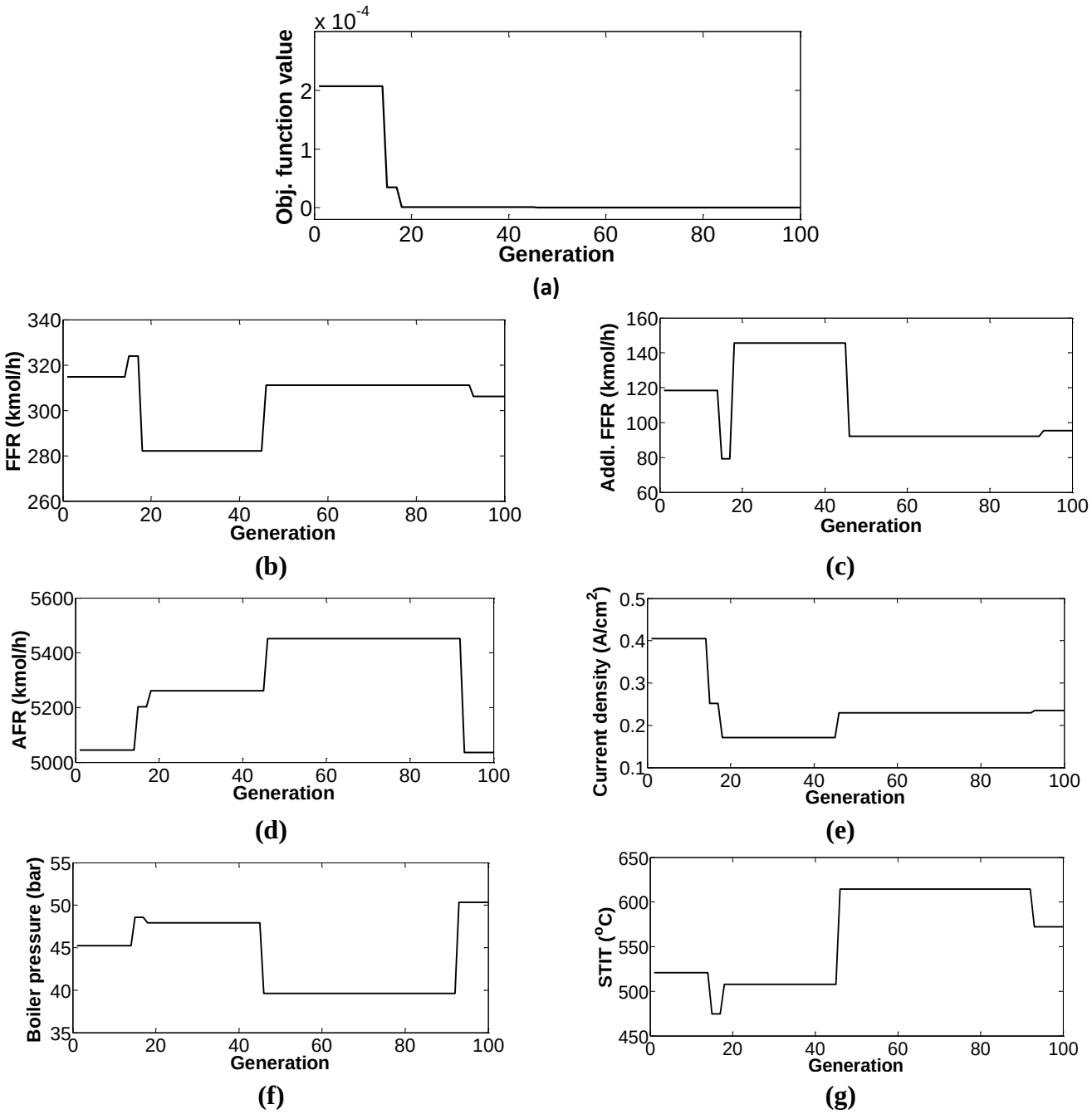

Fig. 4.3: Iterative variation of operating parameters estimated during Run5 (Table 4.3) at CPR 6.

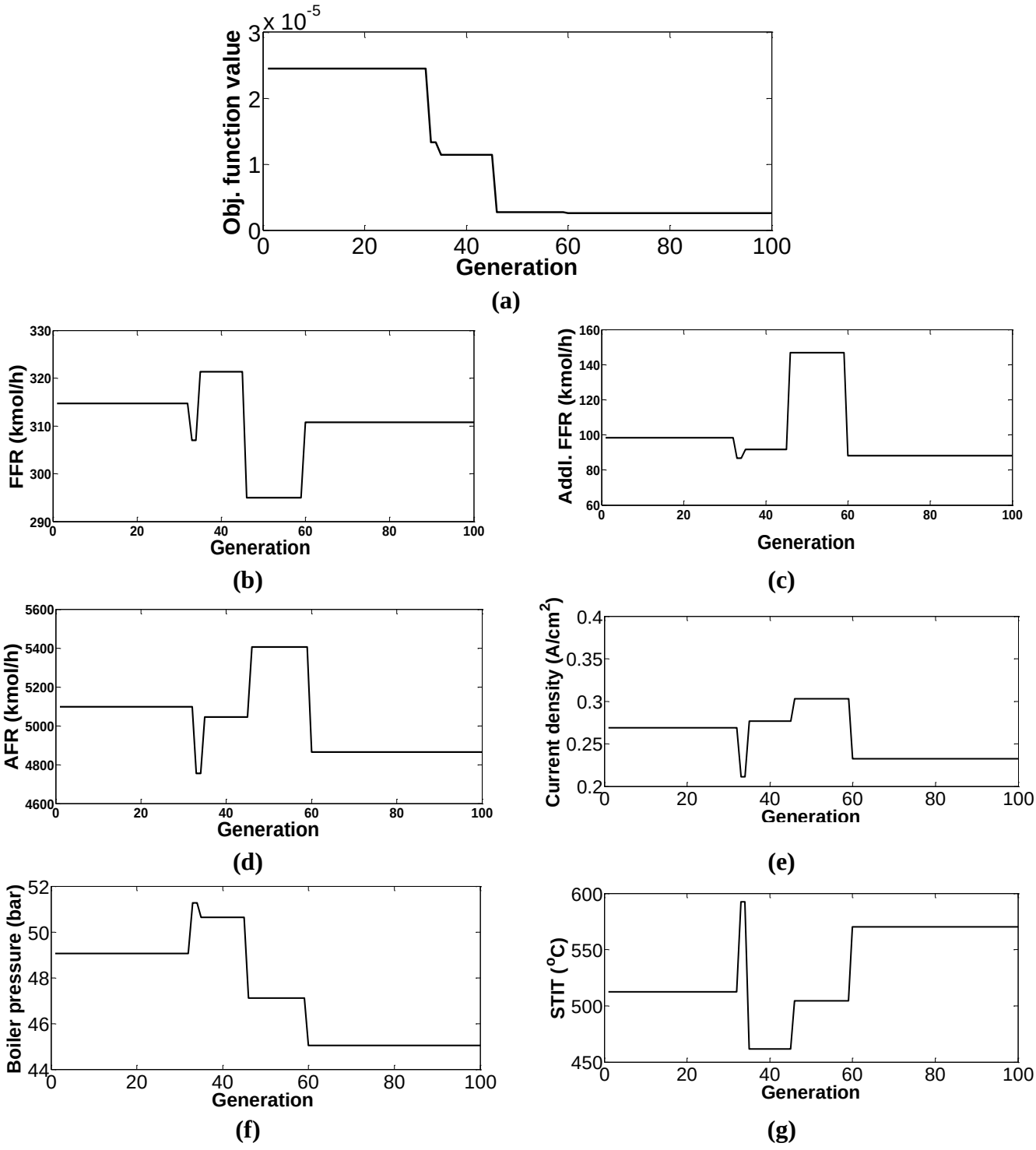

Fig. 4.4: Iterative variation of operating parameters estimated during Run2 (Table 4.3) at CPR 14.

Table 4.4: The values of estimated operating parameters (HRSG pressure, FFR, addl. FFR, AFR, STIT and current density) during five various test runs corresponding to the energy efficiency of 53.607% and 59.522% at CPR 6 and 14 respectively.

Range: [35–60; 275–325; 50–100; 4500–5500; 425–625; 0.1–0.5]

CPR	Runs	BP (bar)	FFR (kmol/h)	Addl. FFR (kmol/h)	AFR (kmol/h)	STIT (°C)	Current density (A/cm^2)	New power (MW)	New exergy efficiency (%)	New irreversibility (MW)
6	Run1	44.33	317.745	114.945	4964.41	487.61	0.204	52.796	52.087	45.140
	Run2	43.28	294.140	88.290	4992.17	559.77	0.214	46.654	52.099	39.722
	Run3	45.99	308.951	79.623	5269.11	453.45	0.190	47.350	52.066	40.498
	Run4	49.58	287.293	81.605	5233.88	478.96	0.148	44.951	52.069	38.440
	Run5	47.56	305.893	114.211	5000.37	533.07	0.188	51.269	52.098	43.838
14	Run1	56.05	323.289	116.567	5188.06	541.94	0.173	59.661	57.756	40.396
	Run2	52.79	312.679	101.164	4932.32	455.39	0.162	56.087	57.731	38.004
	Run3	59.47	290.698	124.341	4878.43	540.92	0.108	56.312	57.756	38.098
	Run4	44.24	312.526	115.218	4794.57	470.55	0.195	58.029	57.746	39.044
	Run5	49.64	303.956	124.919	5006.77	590.25	0.162	58.437	57.774	38.873

ST power increases at higher FFR due to increase in temperature and mass flow rate of the GT exhaust gases at HRSG inlet. The other parameters (BP, STIT, SOFC current density) also are responsible for the change of net power output. The effect of these parameters on power, efficiency and irreversibility were very clearly explained in chapter 3. On the other hand, corresponding to energy efficiency (59.522%) at CPR 14, all combinations of parameters estimated during Run1 to Run5 exactly satisfy the energy efficiency value but with more net power output from the plant. The exact net power, as stated earlier, is 54.3 MW at CPR 14. The exergy efficiency value found from forward plant simulation corresponding to CPR 14 is 57.771% (see Table 4.1) and it is seen that all these combinations of parameters reproduce more or less the same exergy efficiency which however is slightly less for the parameters estimated during Run1 to Run4 and is marginally higher for the parameters estimated during Run5. It is also seen that the total system irreversibility increases proportionally with increase in net power. In spite of high net power, the new total system irreversibility for the parameters estimated during Run1 to Run5 corresponding to CPR 14 is however relatively less because system irreversibility reduces at higher CPR. The iterative variation of the objective function and the operating parameters estimated during Run4 corresponding to CPR 6 and Run5 corresponding to CPR14 are shown in Figs. 4.5 (a-g) and Figs. 4.6 (a-g) respectively.

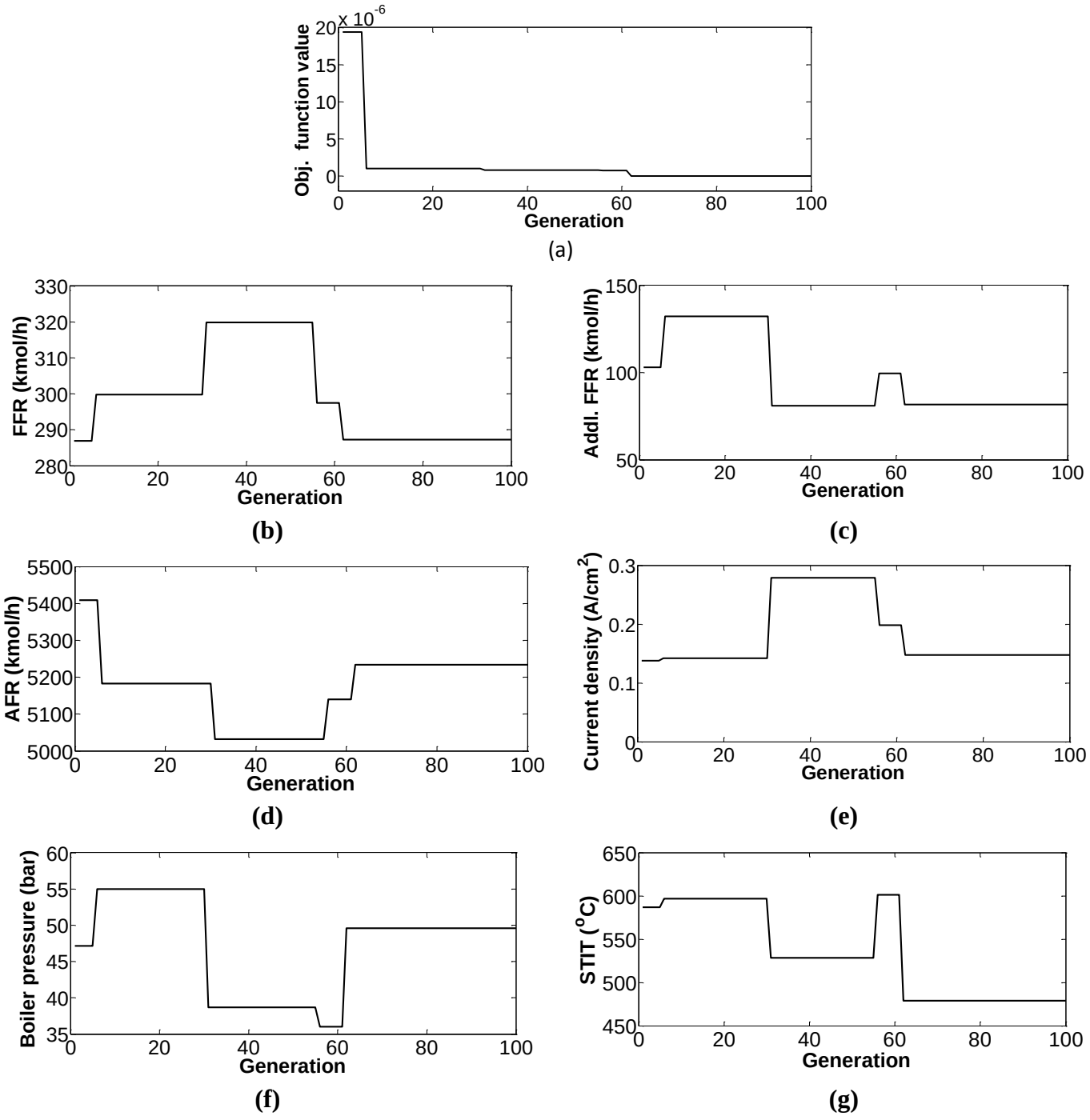

Fig. 4.5: Iterative variation of operating parameters estimated during Run4 (Table 4. 4) at CPR 6.

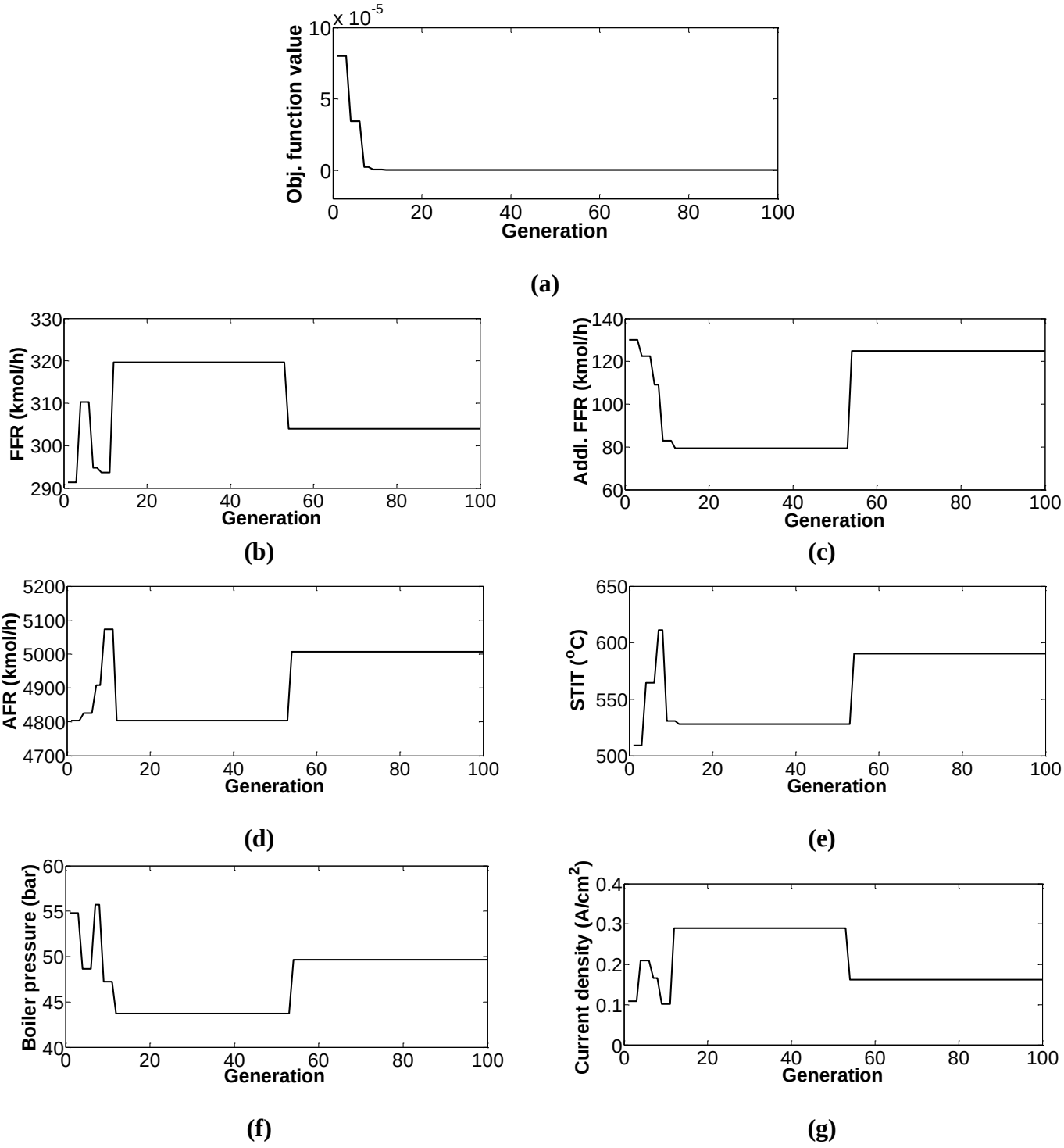

Fig. 4.6: Iterative variation of operating parameters estimated during Run5 (Table 4.4) at CPR 14.

It was seen that the estimated combination of parameters that satisfy a given net power may or may not satisfy the same exact plant efficiencies (energy and exergy)/total system irreversibility obtained from the forward method and gives new efficiencies/irreversibility value either lower or higher than its corresponding exact value. Similarly, parameters that satisfy a given energy efficiency may or may not satisfy the same exact plant net power/exergy efficiency/system irreversibility. Hence, the inverse analysis was also done considering exergy efficiency and total system irreversibility as objective functions separately.

4.3.3 Parameter estimation against a single objective function (Exergy efficiency)

The various combinations of operating parameters estimated with DE based inverse technique corresponding to exergy efficiencies at CPR 6 (52.120%) and 14 (57.771%) are shown in Table 4.5.

Table 4.5: The values of estimated operating parameters (HRSG pressure, FFR, addl. FFR, AFR, STIT and current density) during five various test runs corresponding to the exergy efficiency of 52.120% and 57.771% at CPR 6 and 14 respectively.

Range: [35–60; 275–325; 50–100; 4500–5500; 425–625; 0.1–0.5]

CPR	Runs	BP (bar)	FFR (kmol/h)	Addl. FFR (kmol/h)	AFR (kmol/h)	STIT (°C)	Current density (A/cm^2)	New power (MW	New energy efficiency (%)	New irreversibility (MW)
6	Run1	40.13	314.534	100.313	5466.03	601.08	0.203	50.630	53.615	42.924
	Run2	52.38	281.616	128.588	5264.37	520.161	0.116	50.081	53.635	42.814
	Run3	54.93	278.206	87.982	5104.60	491.23	0.133	44.666	53.658	38.233
	Run4	44.99	301.255	126.775	5295.81	466.795	0.116	52.245	53.646	44.448
	Run5	50.46	306.898	92.942	4897.69	537.82	0.241	48.807	53.635	41.833
14	Run1	52.31	308.513	108.018	4996.45	482.39	0.142	56.496	59.552	38.132
	Run2	46.23	303.495	126.510	4915.95	582.273	0.175	58.372	59.516	39.156
	Run3	45.60	318.373	149.169	5013.34	482.057	0.138	59.538	59.587	42.601
	Run4	49.58	311.572	148.301	4985.05	505.471	0.132	59.535	62.450	41.996
	Run5	46.23	303.495	126.510	4915.95	582.273	0.175	58.372	59.516	39.156

Estimated parameters (Run1-Run5) in both the cases (CPR 6 and CPR 14) exactly satisfy the corresponding exergy efficiencies. In case of exergy efficiency at CPR 6, it was observed that the new net powers reproduced from parameters estimated during Run1, Run2 and Run4 are higher while the power values corresponding to Run3 and Run5 parameters are lower than its exact net power value of 48.85 MW corresponding to CPR 6. Although the new net power values vary from a minimum of 44.666 MW to a maximum of 52.245 MW, but the new energy efficiencies don't change much which are found in the range of 53.615%-53.658%, slightly higher than the exact energy efficiency (53.607%). New total system irreversibility values also vary proportionately with the new net power; the new net power value was the least for the parameters estimated during Run3 at CPR 6 and accordingly the new total system irreversibility was also the minimum.

Similarly corresponding to exergy efficiency at CPR 14 also, it was seen that new net power values derived from the estimated parameters obtained during Run1-Run5 are higher than its corresponding exact net power (54.300 MW). The highest new net power (59.538 MW) was derived from the parameters estimated during Run3. New energy efficiencies were also almost the same with that of the exact energy efficiency (59.522%). Only for the combination of parameters estimated during Run4, the new energy efficiency was higher than the exact value and thus this is a superior combination compared to the others considering that the new net power (59.535 MW) is almost the same with that of the highest new power corresponding to Run3.The iterative variation of the objective function and the operating parameters estimated during Run3 at CPR 6 and Run1 at CPR 14 are shown in Figs. 4.7 (a-g) and Figs. 4.8 (a-g) respectively.

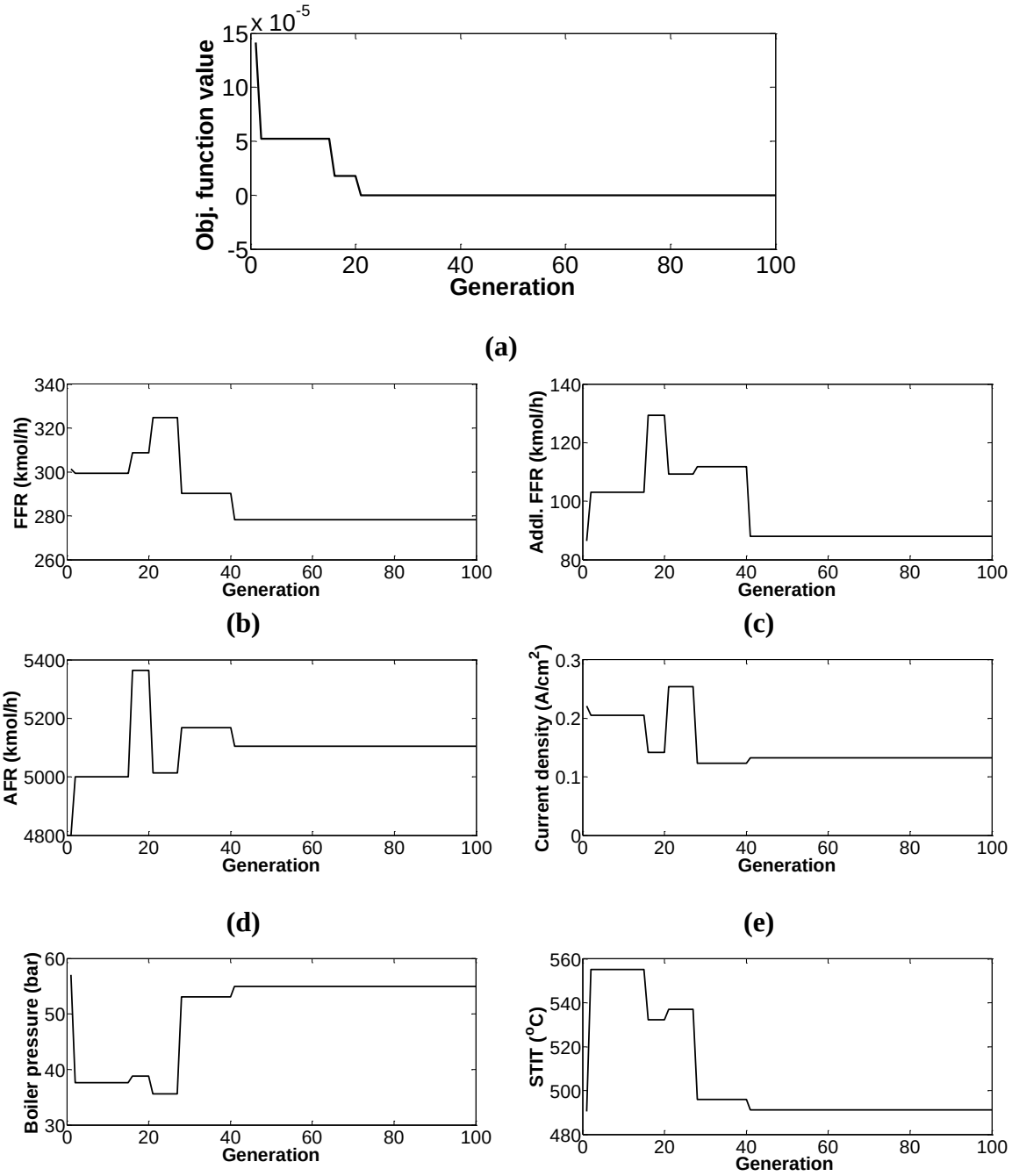

Fig. 4.7: Iterative variation of operating parameters estimated during Run 3 (Table 4.5) at CPR 6.

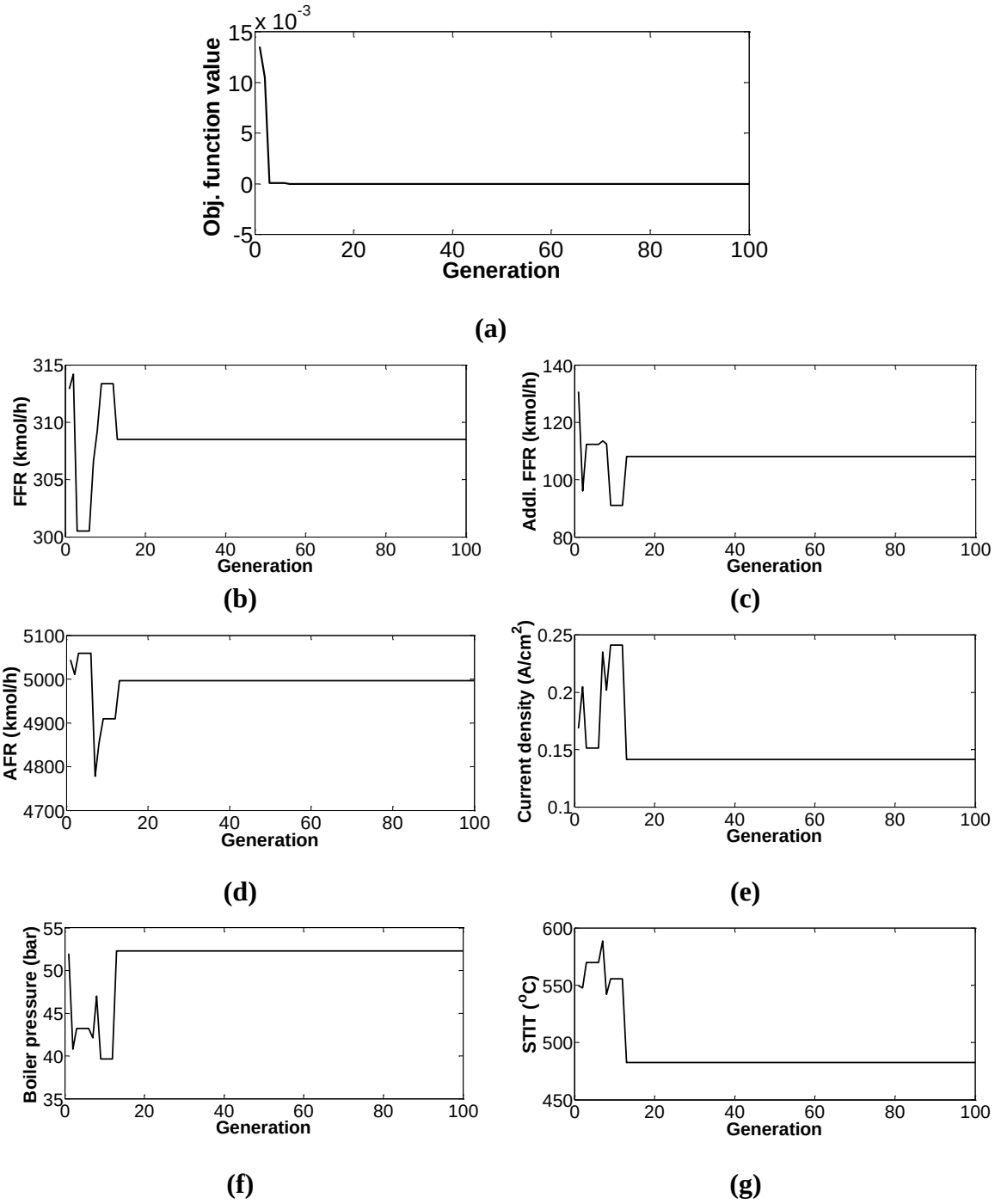

Fig. 4.8: Iterative variation of operating parameters estimated during Run1 (Table 4.5) at CPR 14.

4.3.4 Parameter estimation against a single objective function (Total system irreversibility)

Table 4.6 shows combinations of parameters obtained from inverse method with total system irreversibility at CPR 6 (41.609 MW) and CPR 14 (36.384 MW) as objective functions. Both the objective functions are exactly satisfied by the estimated parameters obtained during Run1-Run5. New net power corresponding to parameters estimated in Run2, Run3 and Run5 are less compared to the exact net power (48.85 MW) while the parameters estimated during Run4 gives slightly higher net power than the exact value. Parameters estimated during Run1 are superior to the others because they upon reproduction give new net power of 55.590 MW which is significantly higher than the exact net power. New energy and exergy efficiency values are also higher than their corresponding exact values. It was mentioned earlier that the total system irreversibility is directly proportional to the net power of the plant. It is now seen from the results obtained during Run1 that the total system irreversibility which is 41.609 MW at CPR 6 corresponding to net power of 48.85 MW, now the plant produces more power with higher energy and exergy efficiency at CPR 6 when it is operated with parameters obtained in Run1. A closer look at these parameters reveal that the total FFR (FFR plus additional FFR), BP and STIT are relatively more while the AFR and SOFC current density are comparatively less for this combination. The STIT upper bound was fixed at 620°C, so the estimated STIT 609.67°C although on the higher side but fall within the investigated range. Maximum permissible STIT of the order of 620°C is possible nowadays with the use of new ST blade materials with improved properties [23].

Similarly with respect to total irreversibility (36.384 MW) at CPR 14, all the estimated combinations of parameters reproduce new net power and efficiencies that are lower than the exact net power (54.300 MW) and exact efficiencies (59.522% and 57.771%) except the parameters estimated during Run3. The new net power and efficiency for this combination of parameters obtained during Run3 are slightly higher than their corresponding exact values. The new net power and efficiencies are more due to comparatively higher values of estimated BP, total FFR and proportionately less AFR. Comparatively lower SOFC current density is also one of the reasons of higher net power. The iterative variation of the objective function and the operating parameters

estimated during Run1 at CPR6 and Run3 at CPR14 are shown in Figs. 4.9 (a-g) and Figs. 4.10 (a-g) respectively.

Table 4.6: The values of estimated operating parameters (HRSG pressure, FFR, addl. FFR, AFR, STIT and current density) during five various test runs corresponding to the total system irreversibility of 41.609 MW and 36.384 MW at CPR 6 and 14 respectively.

Range: [35–60; 275–325; 50–100; 4500–5500; 425–625; 0.1–0.5]

CPR	Runs	BP (bar)	FFR (kmol/h)	Addl. FFR (kmol/h)	AFR (kmol/h)	STIT (◦C)	Current density (A/cm^2)	New power (MW	New energy efficiency (%)	New exergy efficiency (%)
6	Run1	57.41	311.754	115.730	4644.09	609.667	0.128	55.590	57.199	56.059
	Run2	54.81	294.095	84.161	4939.89	523.453	0.302	44.181	51.280	49.839
	Run3	43.56	279.806	102.634	4791.51	507.560	0.248	44.789	51.393	49.958
	Run4	37.70	309.251	95.214	4764.47	425.401	0.209	49.760	54.094	52.540
	Run5	43.61	292.035	77.845	4625.53	496.667	0.461	42.069	49.877	48.489
14	Run1	55.34	295.035	77.713	4794.6	547.296	0.337	48.353	56.891	55.217
	Run2	37.24	287.729	109.881	9918.01	541.12	0.158	53.383	58.895	57.162
	Run3	57.87	324.042	79.781	4867.55	488.43	0.184	55.673	60.608	58.776
	Run4	44.13	317.513	75.919	4897.03	537.14	0.300	52.833	58.954	57.204
	Run5	39.71	285.072	94.124	4819.09	549.41	0.277	49.294	56.983	55.317

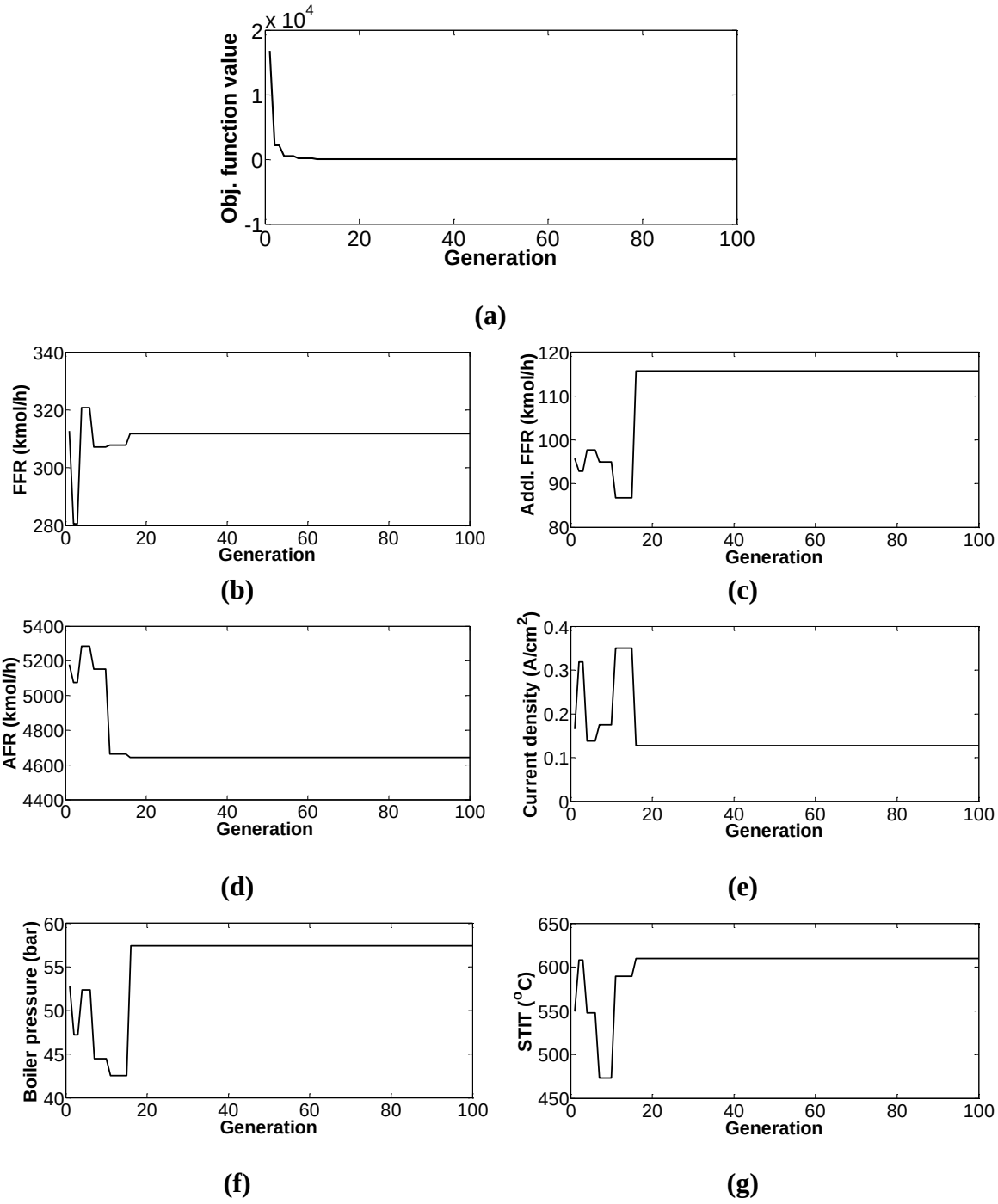

Fig. 4.9: Iterative variation of operating parameters estimated during Run1 (Table 4.6) at CPR 6

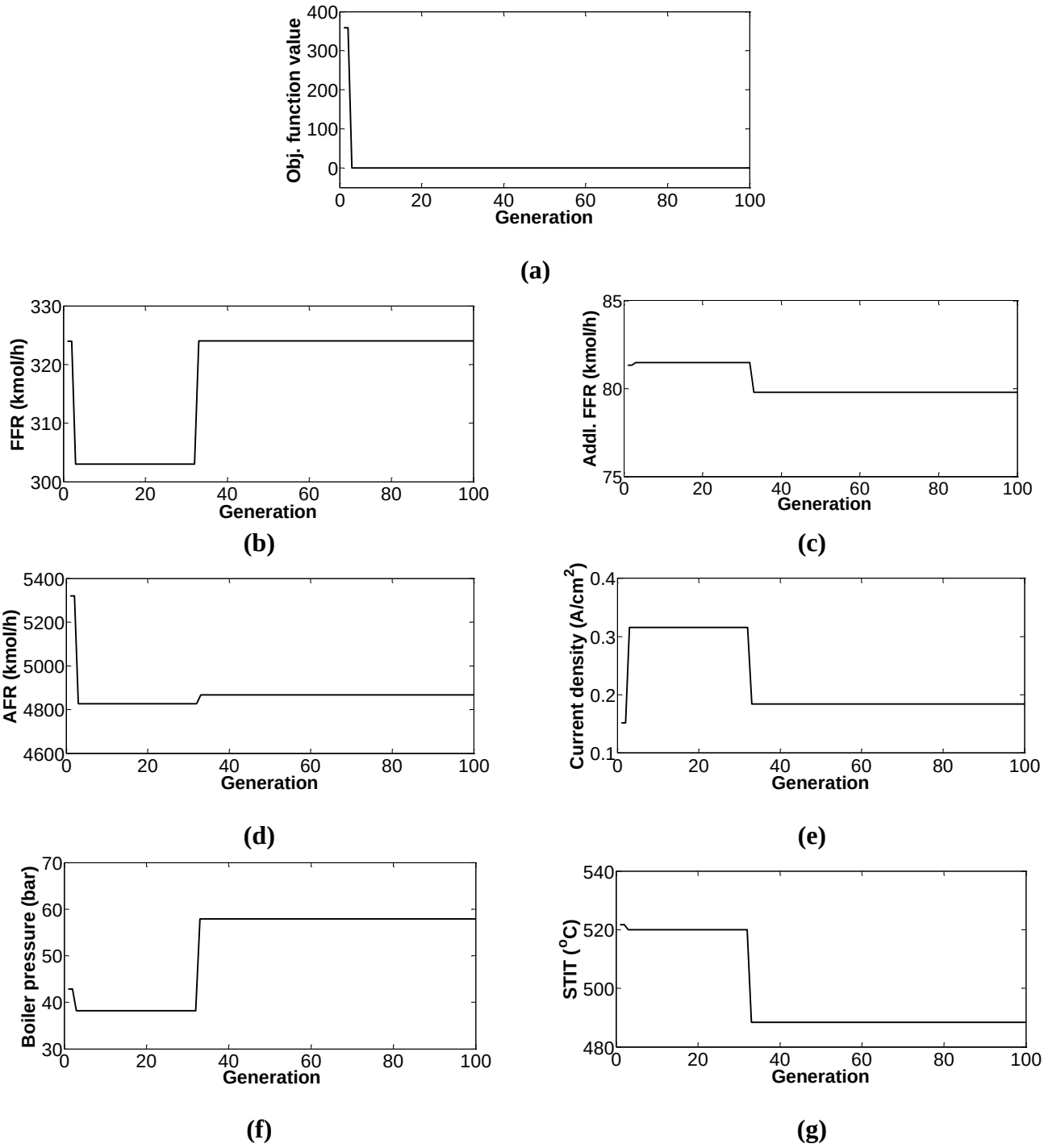

Fig. 4.10: Iterative variation of operating parameters estimated during Run3 (Table 4.6) at CPR 14.

4.3.5 Parameter estimation against an irreversibility value of 36.384 MW at CPR 6

Inverse results corresponding to Run1 with respect to total irreversibility 41.609 MW at CPR 6 and Run3 corresponding to system irreversibility 36.384 MW at CPR 14 in Table 4.6 were found quite interesting. Although it was stated previously that the total system irreversibility is directly linked with the net power, however during the above two estimations at their respective CPR, it was observed that the objective functions of total system irreversibility at CPR 6 and CPR 14 are exactly satisfied but with higher net power output and efficiencies. Moreover, the SOFC integrated combined cycle power system produces more power with higher efficiencies and low total irreversibility at higher CPR. Therefore with this idea, the DE based inverse analysis was done separately considering total irreversibility of 36.384 MW as objective function at CPR 6 which actually is an outcome of the direct simulation at CPR 14 (see Table 4.1). Five test runs were conducted for this case although it is possible to run any number of test runs. The inverse estimations are shown in Table 4.7.

Table 4.7: The values of estimated operating parameters (HRSG pressure, FFR, addl. FFR, AFR, STIT and current density) during five various test runs corresponding to the total system irreversibility of 36.384 MW at CPR 6

Range: [35–60; 275–325; 50–100; 4500–5500; 425–625; 0.1–0.5]

CPR	Runs	BP (bar)	FFR (kmol/h)	Addl. FFR (kmol/h)	AFR (kmol/h)	STIT (°C)	Current density (A/cm^2)	New power (MW	New energy efficiency (%)	New exergy efficiency (%)
6	Run1	49.89	281.129	76.292	5041.14	565.997	0.154	44.448	54.708	53.156
	Run2	46.08	299.569	76.449	4504.01	446.606	0.143	48.846	57.225	55.553
	Run3	42.70	295.651	75.413	5125.22	578.474	0.138	47.345	56.169	54.566
	Run4	57.71	298.730	77.591	4625.46	561.812	0.141	49.158	57.526	55.868
	Run5	54.95	285.373	78.005	5374.44	551.919	0.102	45.728	55.408	53.821

It was seen that the plant which actually produces a net power 48.850 MW at CPR 6 with total system irreversibility 41.609 MW and energy efficiency 53.607% is now giving almost the same net power during Run2 and Run4 with much higher energy efficiency of 57.225% and 57.526% respectively. This is again due to the combination of the parameter values, a direct advantage of the inverse method over the forward simulation method. That multiple combinations of parameters satisfy the same objective function can be shown only through inverse analysis and not possible in the conventional forward based parametric analysis. Likewise, any objective function value be set and the operating parameters can be obtained using the inverse technique. The iterative variation of the objective function and the operating parameters estimated during Run4 is shown in Figs. 4.11 (a-g).

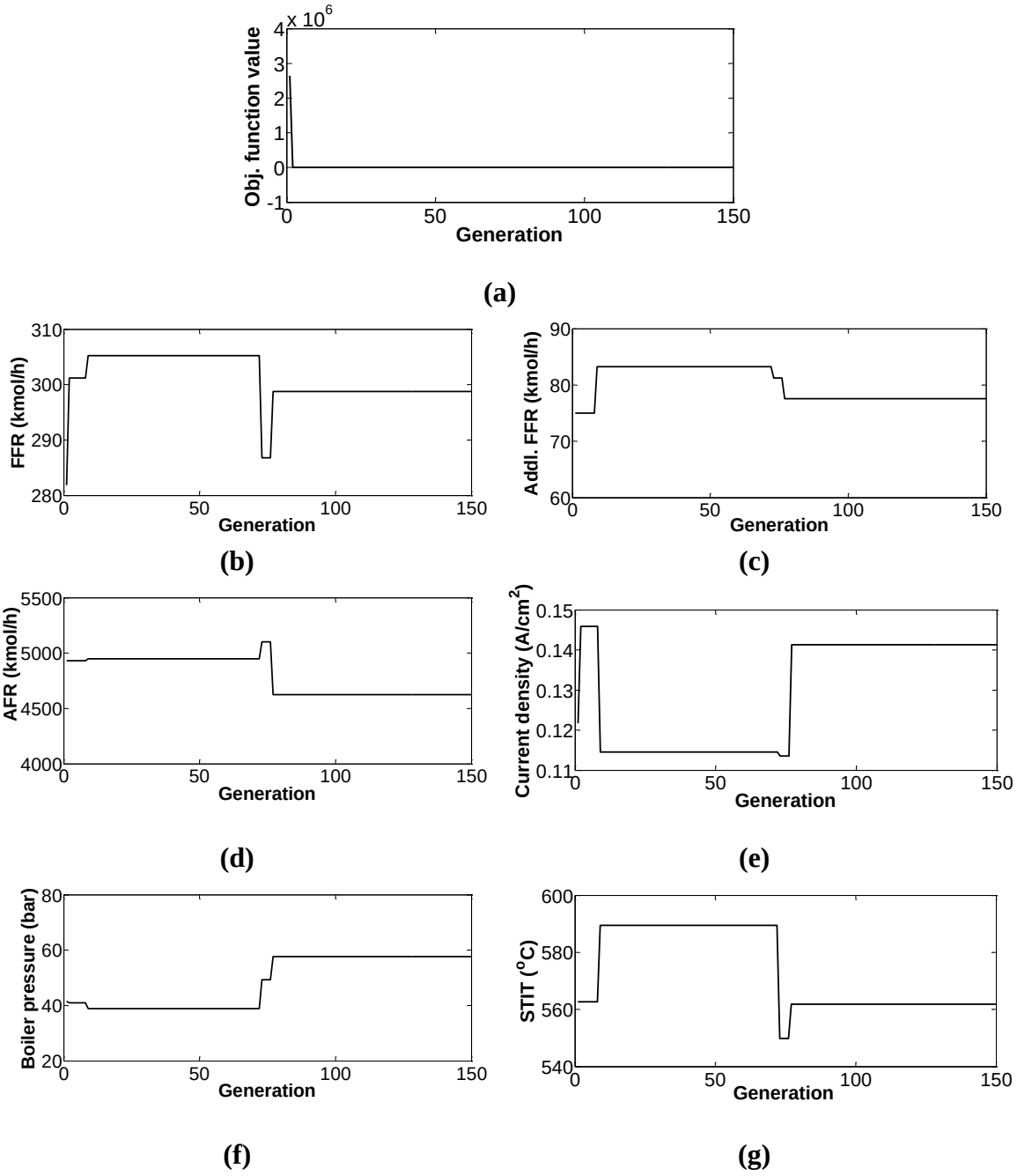

Fig 4.11: Iterative variation of operating parameters estimated during Run4 (Table 4.7) at CPR 6.

4.3.6 Parameter estimation against all four known objective functions at CPR 6 and CPR 14

The unknown operating parameters were also estimated simultaneously against all the four objective functions. The parameters estimated during various test runs corresponding to CPR 6 and 14 are shown in Table 4.8. At each CPR, four set of parameters were estimated during Run1, Run2, Run3 and Run4 considering 100, 150, 200 and 250 numbers of generations respectively. It was seen that the new values of power, efficiencies and total irreversibility obtained with parameters estimated during various runs don't exactly satisfy the objective function values. However, the parameters obtained during Run3 with 200 generations could reproduce almost the same objective function values, particularly the net power and the energy efficiency values both at CPR 6 and 14. And these objective function values at CPR 6 and CPR 14, which are nearly satisfied in all the runs, are actually satisfied by parameter values that are different from those which were considered earlier in the forward analysis.

Table 4.8: The values of estimated operating parameters (HRSG pressure, FFR, addl. FFR, AFR, STIT and current density) during various test runs against the known values of the four objective functions at CPR 6 and 14.

Range: [35–60; 275–325; 50–100; 4500–5500; 425–600; 0.1–0.35]

CPR	Runs	BP (bar)	FFR (kmol/h)	Addl. FFR (kmol/h)	AFR (kmol/h)	STIT (°C)	Current density (A/cm^2)	New power (MW)	New energy efficiency (%)	New exergy efficiency (%)	New total irreversibility (MW)
6	Run1	38.882	310.259	89.981	4628.645	579.110	0.323	48.885	53.635	52.136	41.590
	Run2	40.152	310.896	89.332	4821.709	546.008	0.280	48.852	53.622	52.113	41.600
	Run3	40.219	305.420	94.783	4720.906	567.288	0.275	48.850	53.608	52.108	41.603
	Run4	46.683	300.643	99.678	5238.200	596.984	0.191	48.853	53.612	52.116	41.616
14	Run1	40.830	306.717	93.597	4773.010	533.733	0.237	54.283	59.514	57.748	36.389
	Run2	44.628	308.963	91.644	5130.884	559.940	0.174	54.244	59.460	57.703	36.427
	Run3	40.288	324.188	76.398	5009.625	524.189	0.258	54.297	59.539	57.764	36.385
	Run4	44.755	304.068	95.501	5036.458	519.489	0.154	54.305	59.532	57.765	36.389

4.4 Summary

A DE based inverse algorithm was used for the first time to estimate six operating parameters simultaneously of a SOFC integrated combined GT–ST power cycle. Net power, efficiencies (energy and exergy) and total system irreversibility of the power cycle at CPR 6 and 14 were considered as objective functions. The observations made from the inverse analysis performed on SOFC–GT–ST system can be summarized as follows.

- 100 generations were sufficient for retrieval of a single objective function. In case of parameter estimation against multiple (four) known objectives, however, 100 generations were not sufficient and it would require more than 200 number of generations to exactly satisfy the objective function values.
- Multiple combinations of parameters satisfy a given objective function/set of objective functions and each set of parameters are unique within the prescribed range of lower and upper bound.
- In some of the estimations corresponding to total system irreversibility at CPR 6 and CPR 14, the objective functions were satisfied with higher net power output and efficiencies.
- During estimations corresponding to total irreversibility of 36.384 MW at CPR 6 (which actually was the value at CPR 14 in the forward simulation), the system produced the same exact power of 48.85 MW or higher with parameters obtained during Run2 and Run4 (Table 4.7). The energy and exergy efficiencies with respect to these parameters were also higher than their corresponding exact values.
- DE based inverse technique was quite successful in estimating the operating parameters of a hybrid SOFC–GT–ST plant and better combination of parameters could be obtained from the inverse analysis.

Bibliography

[1] Gogoi, T.K., and Das, R. Inverse analysis of an internal reforming solid oxide fuel cell system using simplex search method. *Applied Mathematical Modelling*, 37:6994–7015, 2013.

[2] Gogoi, T.K. and Das, R. A combined cycle plant with air and fuel recuperator for captive power application. Part 2: Inverse analysis and parameter estimation. *Energy Conversion and Management*, 79:778–789, 2014.

[3] Bhowmik, A., Singla, R. K. , Roy, P. K. , Prasad, D. K., Das, R., Repaka, R. Predicting geometry of rectangular and hyperbolic fin profiles with temperature-dependent thermal properties using decomposition and evolutionary methods. *Energy Conversion and Management*, 74:535–547, 2013.

[4] Parwani, A.K., Talukdar, P., and Subbarao, P.M.V. Performance evaluation of hybrid differential evolution approach for estimation of the strength of a heat source in a radiatively participating medium. *International Journal of Heat Mass Transfer*, 56: 552–560, 2013.

[5] Zentar, R., Hicher, P.Y. and Moulin, G. Identification of soil parameters by inverse analysis. *Computers and Geotechnics*, 28: 129–144, 2001.

[6] Szeliga, D., Gawad, J., and Pietrzyk, M. Inverse analysis for identification of rheological and friction models in metal forming. *Computer Methods in Applied Mechanics and Engineering*, 195: 6778–6798, 2006.

[7] Das, R., Mishra, S. C., Uppaluri, R. Inverse analysis applied to retrieval of parameters and reconstruction of temperature field in a transient conduction–radiation heat transfer problem involving mixed boundary conditions. *International Communications in Heat and Mass Transfer*, 37:52–57, 2010.

[8] Das, R., Mishra, S. C., Ajith, M., and Uppaluri, R. An inverse analysis of a transient 2-D conduction–radiation problem using the lattice Boltzmann method and the finite volume method coupled with the genetic algorithm. *Journal of Quantitative Spectroscopy & Radiative Transfer*, 109:2060–2077, 2008.

[9] Orlande, H.R.B., Fudym, O.,Maillet, D., and Cotta, R.M. *Thermal Measurements and Inverse Techniques.* CRC Press, Taylor & Francis Group, 2011.

[10] De Jong, K.A. *Evolutionary computation: a unified approach*. Cambridge MA: MIT Press, 2006.

[11] Storn, R. and Price, K. Differential evolution – a simple and efficient heuristic for global optimization over continuous space. Journal Glob. Optim. , 11: 341–359, 1997.

[12] Holland, J. H. *Adaptation in Natural Artificial Systems.* University of Michigan Press, 1975.

[13] Gogoi, T. K. , Pandey, M. ,and Das, R. Estimation of operating parameters of a reheat regenerative power cycle using simplex search and differential evolution based inverse methods. *Energy conversion and management*, 91: 204-218, 2015.

[14] Gogoi, T.K. Estimation of Operating Parameters of a Water–LiBr Vapor Absorption Refrigeration System through Inverse Analysis. ASME Journal of Energy Resour. Technol., 138(2): 022002-022002-16, 2015.

[15] Mallipeddi, R., Suganthan, P.N., Pan, Q.K., and Tasgetiren, M.F. Differential evolution algorithm with ensemble of parameters and mutation strategies. Applied Soft Computing, 11:1679–1696, 2011.

[16] Ardia, D., Boudt, K., Carl, P., Mullen, K. M., and Peterson, B. G. Differential Evolution with DEoptim, An Application to Non-Convex Portfolio Optimization. *The R Journal*, 3:27–34, 2011.

[17] Lu, F. and Gao, L. A novel differential evolution algorithm for global search and sensor selection. In *49th IEEE Conference on Decision and Control*, pages 2215 – 2220, Atlanta, USA,2010.

[18] Qin, A.K. and Suganthan, P.N. Self-adaptive Differential Evolution Algorithm for Numerical Optimization. *Evolutionary computation*, 2: 1785−1791, 2005.

[19] Chan, S.H., Ho, H.K., and Tian, Y. Modelling a simple hybrid SOFC and gas turbine plant. *Journal of power sources*, 109:111-120, 2002.

[20] Bavarsad, P. G. Energy and exergy analysis of internal reforming solid oxide fuel cell–gas turbine hybrid system. *International Journal of Hydrogen Energy*, 32: 4591 – 4599, 2007.

[21] Arsalis, A. Thermoeconomic Modeling and Parametric Study of Hybrid Solid Oxide Fuel Cell – Gas Turbine – Steam Turbine Power Plants Ranging from 1.5 MWe to 10 MWe. *Journal of power sources*, 181: 313-326, 2008.

[22] Aminyavari, M., Mamaghani, A. H.,Shirazi, A., Najafi, B., and Rinaldi, F. Exergetic, economic, and environmental evaluations and multi-objective optimization of an internal-reforming SOFC–gas turbine cycle coupled with a Rankine cycle. *Applied Thermal Engineering*, 108:833–846, 2016.

[23] Cengel, Y. A. and Boles, M.A. *Thermodynamics: An Engineering Approach*. Tata McGraw-Hill, 5th edition, 2006.

[24] Haseli, Y., Dincer, I., and Naterer, G.F. Thermodynamic modeling of a gas turbine cycle combined with a solid oxide fuel cell. *International Journal of hydrogen energy*, 33:5811-5822, 2008.